Probabilistic model of resistance jumps in memristive devices

Valeriy A. Slipko*

Institute of Physics, Opole University, Opole 45-052, Poland

Yuriy V. Pershin†

Department of Physics and Astronomy, University of South Carolina, Columbia, South Carolina 29208, USA

(Received 14 February 2023; accepted 15 May 2023; published 16 June 2023)

Resistance switching memory cells such as electrochemical metallization cells and valence change mechanism cells have the potential to revolutionize information processing and storage. However, the creation of *deterministic* resistance switching devices is a challenging problem that is still open. At present, the modeling of resistance switching cells is dominantly based on deterministic models that fail to capture the cycle-to-cycle variability intrinsic to these devices. Herewith we introduce a state probability distribution function and associated integrodifferential equation to describe the switching process consisting of a set of stochastic jumps. Numerical and analytical solutions of the equation have been found in two model cases. This work expands the toolbox of models available for resistance switching cells and related devices and enables a rigorous description of intrinsic physical behavior not available in other models.

DOI: 10.1103/PhysRevE.107.064117

I. INTRODUCTION

Resistance switching memory cells (also known as memristive devices [1]) are emerging components with memory that find applications in neuromorphic [2–4], logic [5,6], and reservoir computing circuits [7], to name a few. Since the early 2010s, significant progress has been achieved in the above-mentioned and related areas and includes the demonstration of high-density crossbar arrays [8], diffusive memristors [9], etc. Moreover, the utilization of natural materials and unconventional fabrication techniques [10] may lead to memory cells that have a lower carbon footprint compared to silicon-based electronics.

Traditionally, memristive devices have been described in terms of deterministic models. The dynamical system approach introduced by Chua and Kang [1] provides the mainstream theoretical framework (examples of memristive models can be found in Refs. [11–13]). However, being relatively simple, deterministic models neglect the stochastic behavior in particular common to electrochemical metallization (ECM) cells [14] and valence change mechanism (VCM) cells [15]—the most typical memristive devices. As an example, Fig. 1 shows the current-voltage curve for $Cu/AlO_x/W$ nonvolatile memory structure [16].

In the present paper, we develop a continuous probabilistic model to describe the evolution of stochastic memristive devices. The main assumption in the model is that the resistance switching occurs via random Markovian jumps in the continuous space of internal state variable(s). Previously, we have pioneered the use of a master equation as a tool for examining the response of stochastic memristive devices with discrete states [17], implemented this approach in SPICE [18], and developed a theory of circuits combining discrete stochastic memristive devices with reactive components [19]. Recently, the master equation was used in the analysis of memristive Ising circuits [20], which are the electronic circuit realization of the Ising model. The present paper extends the discrete master equation approach [17,18,21] to a more realistic case of continuous internal states [22].

II. MODEL

To take into account the stochasticity, we introduce the state probability distribution function $p(x,t)$, where $x \in [a,b]$ is the internal state variable responsible for memory, and $p(x,t)dx$ is the probability to find the state in the interval from x to $x+dx$ at the time moment t. The state probability distribution function is normalized to 1:

$$\int_a^b p(x,t)dx = 1. \tag{1}$$

The first equation in the model is a statistically averaged Ohm's law

$$\langle I\rangle = \left\langle \frac{V}{R(x,V)} \right\rangle \equiv \overline{R}^{-1}(V)V, \tag{2}$$

where $\langle I\rangle$ is the mean current, V is the voltage across the device, $R(x,V)$ is the state- and voltage-depend resistance, and $\overline{R}(V) = (\int_a^b R^{-1}(x,V)p(x,t)dx)^{-1}$ is the harmonic mean resistance. We emphasize that $\overline{R}(V) \neq \langle R(x,V)\rangle$.

The evolution of $p(x,t)$ is represented by an integrodifferential equation

$$\frac{\partial p(x,t)}{\partial t} = \int_a^b \gamma(x',x,V(x'))p(x',t)dx' - p(x,t)\int_a^b \gamma(x,x',V(x))dx', \tag{3}$$

*vslipko@uni.opole.pl

†pershin@physics.sc.edu

 ©2023 American Physical Society

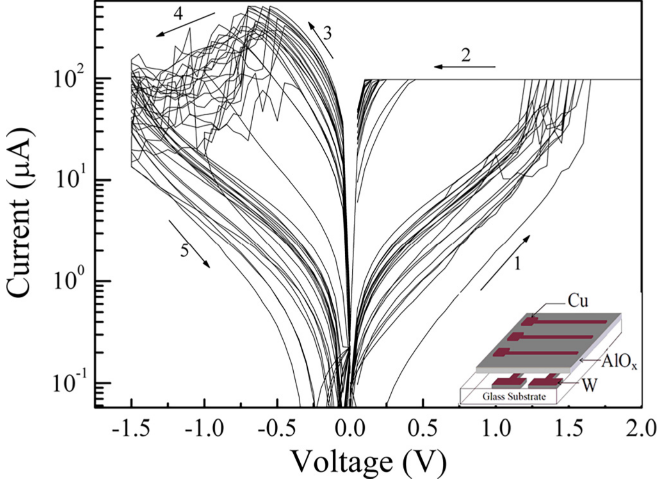

FIG. 1. Experimental current-voltage curves of Cu/AlO_x/W nonvolatile memory structure (for details, see Ref. [16]). Reprinted from Ref. [16].

which is the second equation in the model. Here $\gamma(y, z, V(y))$ is the voltage-dependent transition rate density from internal state y to z, and $V(y)$ is the voltage across the device in state y. The first term in the right-hand side of (3) describes the transitions to x from all other states, while the second one describes the reverse transitions.

The extension of Eqs. (2) and (3) to several internal state variables is discussed in Supplemental Material [22].

To illustrate the above model, we consider two special cases of Eqs. (2) and (3). In both cases, we will use the resistance $R \in [R_{on}, R_{off}]$ as the internal state variable, $x \equiv R$, and the resistance probability distribution function, $r(R, t)$, as the state probability distribution function. Here R_{on} and R_{off} denote the ON and OFF state resistance, respectively.

III. UNIFORM DISTRIBUTION OF JUMPS

In the first model, we assume a uniform continuous distribution of jumps in the direction defined by the applied voltage. The transition rate density in Eq. (3) is selected as

$$\gamma(R', R, V) = \begin{cases} \alpha_{10} e^{\frac{|V|}{V_{10}}}, & V > 0,\ R' < R \\ \alpha_{01} e^{\frac{|V|}{V_{01}}}, & V < 0,\ R' > R \\ 0, & \text{otherwise} \end{cases}, \tag{4}$$

where α_{10}, V_{10}, and α_{01}, V_{01} are the coefficients defining the transition rates in the direction from the ON to OFF (10) and OFF to ON (01) resistance states, respectively. In Eq. (4) and Eq. (9), the exponential dependence of the switching rate on the voltage was introduced phenomenologically inspired by the experimental observations published in Refs. [23–25]. In particular, the studies of Ag/a-Si/p-Si pillar ECM devices [23] subjected to constant voltage have revealed that the occupation probability of the initial state decays exponentially with the decay time depending exponentially on the voltage, $\tau(V) = \tau_0 \exp(-V/V_0)$. The same exponential dependence was observed in the cross-bar ECM devices based on the same material combination [24] as well as in ZrO_x-based VCM devices [25]. While in the above-mentioned ECM devices [23,24] the characteristic times were in milliseconds, in VCM devices [25] the times were in microseconds. As Eqs. (4) and (9) are written for the rates, there is no minus sign in front of the voltage. Below, we use the notation $\gamma_{10} = \alpha_{10}\exp(|V|/V_{10})$ corresponding to the top line in the right-hand side of Eq. (4).

Figure 2 shows results of numerical simulations for the above model in the case of sinusoidal driving. We note that the frequency behavior of current-voltage curves in Fig. 2(a) is typical to memristive devices. Within each period, the maximum of the resistance distribution function $r(R, t)$ drifts from R_{ON} to R_{OFF} and back. Note that Fig. 2(c) shows the evolution in the first half-period of periodic driving. Figures 2(d)– 2(f) demonstrate that the resistance distribution function becomes more localized at higher frequencies. Overall, all these results are not unexpected.

Next, we simulate the response to step voltage (Fig. 3). According to Fig. 3(a), the step voltage switches the resistance from R_{on} to R_{off} in a relatively short time interval. A notable feature is the exponential decay in the resistance probability distribution function as seen in the bottom panel in Fig. 3(b).

The analytical solution of Eq. (3) with γ given by Eq. (4) and $V = \text{const}$ can be found using the method of Laplace transform. One can show (see Supplemental Material [22]) that the general solution for $V > 0$ can be written as

$$r(R, t) = \gamma_{10} t e^{-\gamma_{10}(R_{off}-R)t} \int_{R_{on}}^{R} r(R', 0) dR' + r(R, 0) e^{-\gamma_{10}(R_{off}-R)t}, \tag{5}$$

where $r(R, 0)$ is the initial resistance probability distribution function.

The simple form of the general solution (5) allows the detailed analysis of the evolution for any initial resistance probability distribution function $r(R, 0)$. Consider, for instance, $r(R, 0) = \delta(R - R_{on})$ (the detailed analysis of this case is given in Supplemental Material [22]). One can easily see that the probability distribution function decreases purely exponentially at the left edge of the distribution (at $R = R_{on}$) with the highest possible rate $\gamma_{10}(R_{off} - R_{on})$:

$$r(R_{on}, t) = r(R_{on}, 0) e^{-\gamma_{10}(R_{off}-R_{on})t}. \tag{6}$$

At the right edge of the resistance interval, the resistance probability distribution finction growths linearly from $t = 0$:

$$r(R_{off}, t) = r(R_{off}, 0) + \gamma_{10} t. \tag{7}$$

This result corresponds to the fact that at the positive voltage, the resistance can only increase (or stay constant), see Eq. (4). This leads to the accumulation of the probability density at $R = R_{off}$. It also follows directly from Eq. (5) that inside of the interval $[R_{on}, R_{off}]$, $r(R, t)$ increases first and then decreases. The decrease is exponential with R-dependent rate $\gamma_{10}(R_{off} - R)$. Moreover, the linear growth of probability (7) at R_{off} implies that the characteristic width of the distribution peak decreases as $(\gamma_{10} t)^{-1}$ asymptotically in time.

Equation (5) allows finding various quantities on average such as the mean resistance

$$\langle R \rangle(t) = R_{off} - \frac{1 - e^{-\gamma_{10}(R_{off}-R_{on})t}}{\gamma_{10} t} \tag{8}$$

and its variance (see Supplemental Material [22]).

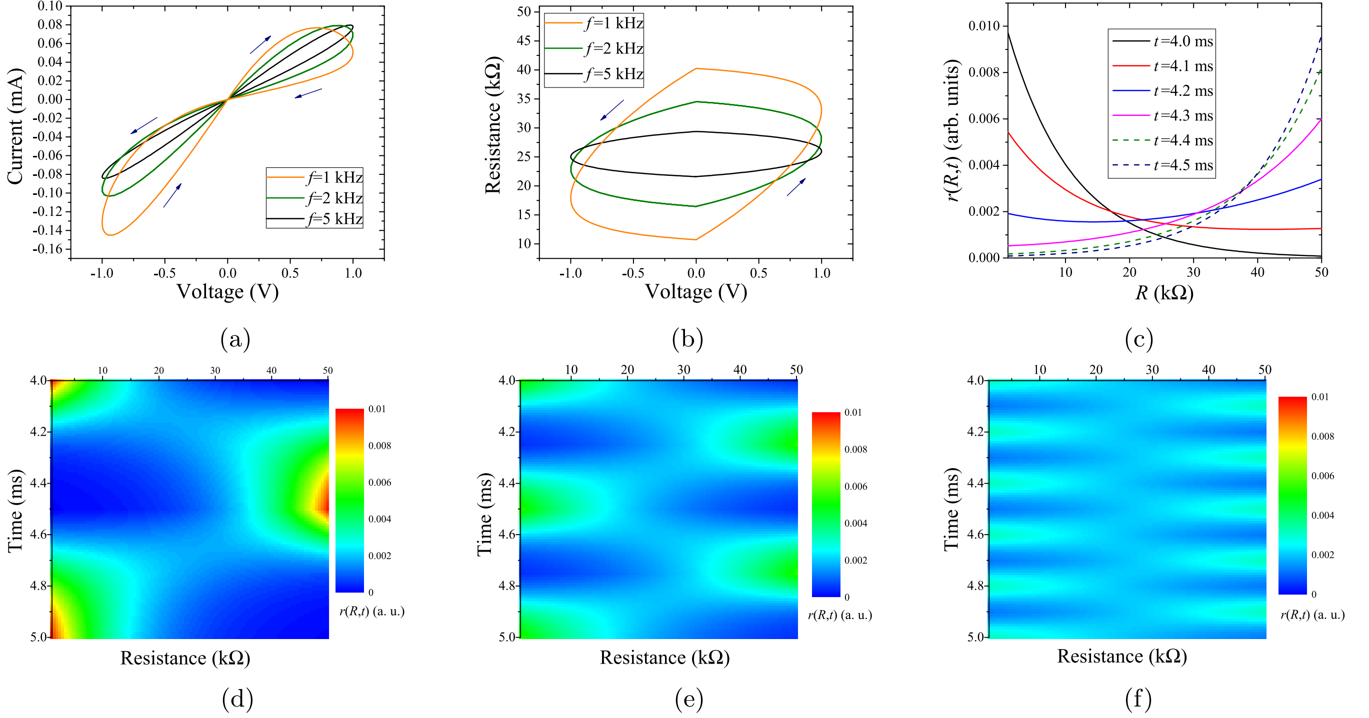

FIG. 2. First model simulations. Response to a sinusoidal voltage $V = V_0 \sin(2\pi f t)$: (a) mean current-voltage curves, (b) $\langle R\rangle(t)$ versus voltage, (c) resistance distribution function at selected times ($f = 1$ kHz), and [(d)–(f)] color plots of $r(R, t)$ at $f = 1, 2, 5$ kHz, respectively. This figure was obtained using the following parameter values: $R_{\text{on}} = 1$ kΩ, $R_{\text{off}} = 50$ kΩ, $\alpha_{10} = \alpha_{01} = 0.1$ $(\text{s} \cdot \Omega)^{-1}$, and $V_{10} = V_{01} = V_0 = 1$ V.

IV. EXPONENTIAL DISTRIBUTION OF JUMPS

In the second model we use R-dependent transition rates to describe the situation when the shorter jumps are more frequent than longer. The transition rate density is selected as

$$\gamma(R, R', V) = \begin{cases} \alpha_{10} e^{\frac{|V|}{V_{10}} - \frac{|R-R'|}{R_0}}, & V > 0,\ R < R' \\ \alpha_{01} e^{\frac{|V|}{V_{01}} - \frac{|R-R'|}{R_0}}, & V < 0,\ R > R', \\ 0, & \text{otherwise} \end{cases} \tag{9}$$

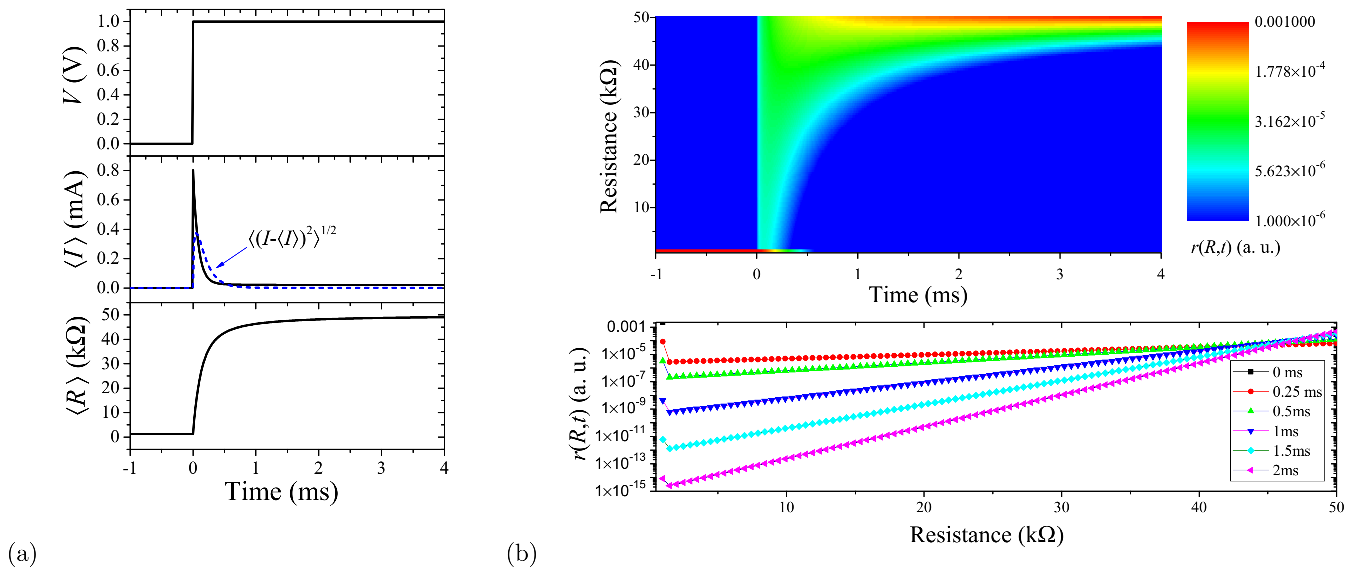

FIG. 3. First model simulations. Response to a steplike voltage: (a) Voltage, mean current, and mean resistance as functions of time and (b) color plot (log scale) of $r(R, t)$ (top) and $r(R, t)$ at selected times (bottom). This figure was obtained using the same parameter values as in Fig. 2 and $r(R, 0) = \delta(R - R_{\text{on}})$.

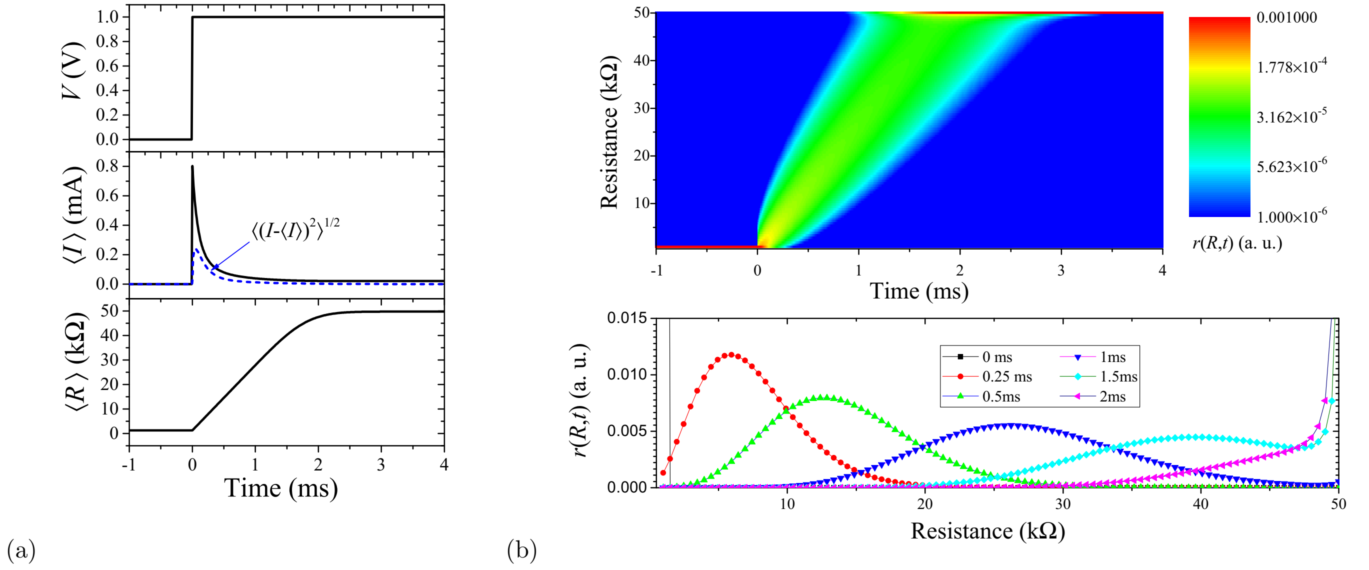

FIG. 4. Second model simulations. Response to a steplike voltage: (a) Voltage, mean current, and mean resistance as functions of time and (b) color plot (log scale) of $r(R,t)$ (top) and $r(R,t)$ at selected times (bottom). This figure was obtained using the following parameter values: $R_{on} = 1$ kΩ, $R_{off} = 50$ kΩ, $\alpha_{10} = \alpha_{01} = 10$ $(\text{s}\cdot\Omega)^{-1}$, $V_{10} = V_{01} = 1$ V, $R_0 = 1$ kΩ, and $r(R,0) = \delta(R - R_{on})$.

where R_0 defines the average size of the jump. In fact, the first model can be considered as the limiting case of the second model in the limit of $R_0 \to \infty$. We note that the parameters in Eqs. (4) and (9) can be in principle derived using molecular dynamics simulations of the resistance switching process.

Figure 4 shows the response of the second model to step voltage. We highlight a couple of interesting features of this result. First, unlike Fig. 3(a), in Fig. 4(a) there is a significant interval of the linear growth of resistance (from 0 to 1.5 ms). Second, the resistance probability distribution function is more localized: In the bottom panel of Fig. 4(b) there is a clear peak that shifts from left to right as the resistance switches from R_{on} to R_{off}.

Compared to the first model, the analytic analysis of the second one is more involved. Its general solution is complex [we give it in Supplemental Material [22], see Eq. (S.17) supplemented by Eq. (S.18)]. This exact analytical solution allows the efficient numerical calculation of the resistance probability distribution function $r(R,t)$ at any moment of time for the whole range of parameters, in particular for small values of R_0. Moreover, it allows the derivation of simple asymptotic formulas for interesting limiting cases.

In particular, the solution for $r(R,0) = \delta(R - R_{on})$ [given by Eq. (S.22) in Supplemental Material [22]] allows us to calculate directly the mean resistance and its variance *at short times*,

$$\langle R\rangle = R_{on} + R_0^2\gamma_{10}t, \tag{10}$$

and

$$\langle (R - \langle R\rangle)^2\rangle = 2R_0^3\gamma_{10}t. \tag{11}$$

In fact, Eqs. (10) and (11) are exact in the limit of $R_{off} \to \infty$ in Eq. (S.22). Note that Eq. (10) explains the linear increase of $\langle R\rangle$ in Fig. 4(a).

Additionally, if $\gamma_{10}t(R - R_{on}) = \gamma_{10}R_0t\xi \gg 1$, then the solution (S.22) can be simplified to

$$r(R,t) = \frac{(\gamma_{10}R_0t)^{1/4}}{2\sqrt{\pi}\xi^{3/4}R_0}e^{-(\sqrt{\xi}-\sqrt{\gamma_{10}R_0t})^2}, \tag{12}$$

where, for shortness, we have introduced $\xi = (R - R_{on})/R_0$.

From Eq. (12) we see that far from both boundaries, R_{on} and R_{off}, the resistance probability distribution function $r(R,t)$ tends asymptotically to the bell-shaped distribution [Eq. (12)] at $t \gg 1/(\gamma_{10}R_0\xi)$. The location of the maximum, $\xi_{max} = \xi_{max}(t)$, can be easily calculated from Eq. (12). At long times, $\gamma_{10}R_0t \gg 1$, we find that $\xi_{max}(t) = \gamma_{10}R_0t - 3/2 + O(1/t)$. It means that in this regime the distribution maximum, ξ_{max}, propagates at constant velocity $\gamma_{10}R_0^2$ in the R space. The magnitude of the distribution maximum $r(\xi_{max}(t),t) = 1/(2R_0\sqrt{\pi\gamma_{10}R_0t})[1 + O(1/t)]$ decreases as the inverse square root of time. This also means that the characteristic width of the probability distribution increases as the square root of time (to satisfy the normalization condition). Another way to see it is to expand up to quadratic terms with respect to $(\xi - \xi_{max})$ the logarithm of Eq. (12). This way we get the following approximated expression for the probability distribution function (12), which is valid in the vicinity of the maximum point $\xi_{max}(t)$ when $\gamma_{10}R_0t \gg 1$:

$$r(R,t) = \frac{1}{2R_0\sqrt{\pi\gamma_{10}R_0t}}e^{-\frac{(\xi-\gamma_{10}R_0t+3/2)^2}{4\gamma_{10}R_0t}}. \tag{13}$$

Equation (13) is the Gaussian distribution with the maximum at $\xi_{max} \approx \gamma_{10}R_0t - 3/2$ and standard deviation $\sqrt{2\gamma_{10}R_0t}$.

Thus we see that the evolution of the initial delta function distribution $r(R,t) = \delta(R - R_{on})$ involves three stages (when $|R_{off} - R_{on}| \gg R_0$). At the first stage, $0 < t \lesssim (\gamma_{10}R_0)^{-1}$, the "running wave", which is described by the second term in Eq. (S.22), is formed near R_{on}. At the second stage, $(\gamma_{10}R_0)^{-1} \lesssim t \lesssim (R_{off} - R_{on})/(\gamma_{10}R_0^2)$, as the first term in

Eq. (S.22) becomes exponentially small, the second term, which can be approximated by Eq. (12), describes the propagation of the "wave" at constant velocity $\gamma_{10}R_0^2$ and its broadening as $2R_0\sqrt{\pi\gamma_{10}R_0t}$ in R space. At the beginning of the last third stage of evolution, $t \gtrsim (R_{\rm off} - R_{\rm on})/(\gamma_{10}R_0^2)$, the "wave" reaches $R_{\rm off}$. At this moment of time, the probability distribution has a characteristic width of $2\sqrt{\pi R_0(R_{\rm off} - R_{\rm on})}$, which is much larger than R_0 [by a factor of $\sim 2\sqrt{\pi(R_{\rm off} - R_{\rm on})/R_0} \gg 1$], and, at the same time, much smaller than $(R_{\rm off} - R_{\rm on})$. Therefore, the probability distribution stays localized the whole evolution time. Eventually, the magnitude of the probability distribution at $R_{\rm off}$ starts to grow linearly in time, $r(R_{\rm off}, t) \sim \gamma_{10}t$, as it follows from the asymptotic behavior of Laplace transform $\tilde{r}(R_{\rm off}, p) \sim \gamma_{10}/p^2$ when $p \to 0$. At the same time, the probability distribution approaches the delta function $\delta(R - R_{\rm off})$.

V. CONCLUSION

In conclusion, we have developed a fundamentally different probabilistic model of memristive devices that takes into account the cycle-to-cycle variability in their response. Our model differs conceptually from the conventional memristive models [26] (even though they may use the transition rates [27]) in its statistical approach to the description of resistance switching phenomenon. Overall, this work provides a new tool for the analysis of stochastic memristive devices and their circuits, and may find applications in other cases, such as the random memristive networks [28], albeit in a modified form.

[1] L. O. Chua and S. M. Kang, Proc. IEEE **64**, 209 (1976).
[2] Y. Li, Z. Wang, R. Midya, Q. Xia, and J. J. Yang, J. Phys. D: Appl. Phys. **51**, 503002 (2018).
[3] Q. Xia and J. J. Yang, Nat. Mater. **18**, 309 (2019).
[4] D. V. Christensen, R. Dittmann, B. Linares-Barranco, A. Sebastian, M. L. Gallo, A. Redaelli, S. Slesazeck, T. Mikolajick, S. Spiga, S. Menzel, I. Valov, G. Milano, C. Ricciardi, S.-J. Liang, F. Miao, M. Lanza, T. J. Quill, S. T. Keene, A. Salleo, J. Grollier *et al.*, Neuromorph. Comput. Eng. **2**, 022501 (2022).
[5] I. Vourkas and G. C. Sirakoulis, IEEE Circ. Syst. Mag. **16**, 15 (2016).
[6] A. Sebastian, M. Le Gallo, R. Khaddam-Aljameh, and E. Eleftheriou, Nat. Nanotechnol. **15**, 529 (2020).
[7] M. S. Kulkarni and C. Teuscher, in *Proceedings of the IEEE/ACM International Symposium on Nanoscale Architectures (NANOARCH'12)* (ACM, New York, NY, USA, 2012), pp. 226–232.
[8] S. Pi, C. Li, H. Jiang, W. Xia, H. Xin, J. J. Yang, and Q. Xia, Nat. Nanotechnol. **14**, 35 (2019).
[9] Z. Wang, S. Joshi, S. E. Savel'ev, H. Jiang, R. Midya, P. Lin, M. Hu, N. Ge, J. P. Strachan, Z. Li *et al.*, Nat. Mater. **16**, 101 (2017).
[10] J. Kim, V. J. Dowling, T. Datta, and Y. V. Pershin, Phys. Stat. Solidi (a) **220**, 2200643 (2022).
[11] S. Kvatinsky, M. Ramadan, E. G. Friedman, and A. Kolodny, IEEE Trans. Circ. Syst. II: Expr. Briefs **62**, 786 (2015).
[12] J. P. Strachan, A. C. Torrezan, F. Miao, M. D. Pickett, J. J. Yang, W. Yi, G. Medeiros-Ribeiro, and R. S. Williams, IEEE Trans. Electr. Dev. **60**, 2194 (2013).
[13] Y. V. Pershin and M. Di Ventra, Adv. Phys. **60**, 145 (2011).
[14] I. Valov, R. Waser, J. R. Jameson, and M. N. Kozicki, Nanotechnology **22**, 254003 (2011).
[15] J. J. Yang, I. H. Inoue, T. Mikolajick, and C. S. Hwang, MRS Bull. **37**, 131 (2012).
[16] A. Sleiman, P. W. Sayers, and M. F. Mabrook, J. Appl. Phys. **113**, 164506 (2013).
[17] V. J. Dowling, V. A. Slipko, and Y. V. Pershin, Chaos, Solitons Fract. **142**, 110385 (2021).
[18] V. Dowling, V. Slipko, and Y. Pershin, Radioengineering **30**, 157 (2021).
[19] V. A. Slipko and Y. V. Pershin, IEEE Trans. Circ. Syst. II: Expr. Briefs **69**, 214 (2021).
[20] V. J. Dowling and Y. V. Pershin, Phys. Rev. E **106**, 054156 (2022).
[21] V. Ntinas, A. Rubio, and G. C. Sirakoulis, IEEE Access **9**, 983 (2021).
[22] See Supplemental Material at http://link.aps.org/supplemental/10.1103/PhysRevE.107.064117 for derivation details and discussion of parasitic capacitance effects, which includes Refs. [11,19,29–31].
[23] S. H. Jo, K.-H. Kim, and W. Lu, Nano Lett. **9**, 496 (2009).
[24] S. Gaba, P. Sheridan, J. Zhou, S. Choi, and W. Lu, Nanoscale **5**, 5872 (2013).
[25] R. Naous, A. Siemon, M. Schulten, H. Alahmadi, A. Kindsmüller, M. Lübben, A. Heittmann, R. Waser, K. N. Salama, and S. Menzel, Sci. Rep. **11**, 4218 (2021).
[26] E. Miranda, G. Milano, and C. Ricciardi, IEEE Trans. Nanotechnol. **19**, 609 (2020).
[27] J. E. Carroll, *Rate Equations in Semiconductor Electronics* (Cambridge University Press, Cambridge, UK, 1990).
[28] F. Caravelli, G. Milano, C. Ricciardi, and Z. Kuncic, Ann. Phys. (Berlin) **2023**, 2300090 (2023).
[29] S. Kvatinsky, E. G. Friedman, A. Kolodny, and U. C. Weiser, IEEE Trans. Circ. Syst. I: Regul. Pap. **60**, 211 (2012).
[30] S. Liu, N. Wu, A. Ignatiev, and J. Li, J. Appl. Phys. **100**, 056101 (2006).
[31] M. Di Ventra, Y. V. Pershin, and L. O. Chua, Proc. IEEE **97**, 1717 (2009).